Lab on a Chip

Miniaturisation for chemistry, physics, biology, & bioengineering

www.rsc.org/loc

Volume 9 | Number 20 | 21 October 2009 | Pages 2861–3024

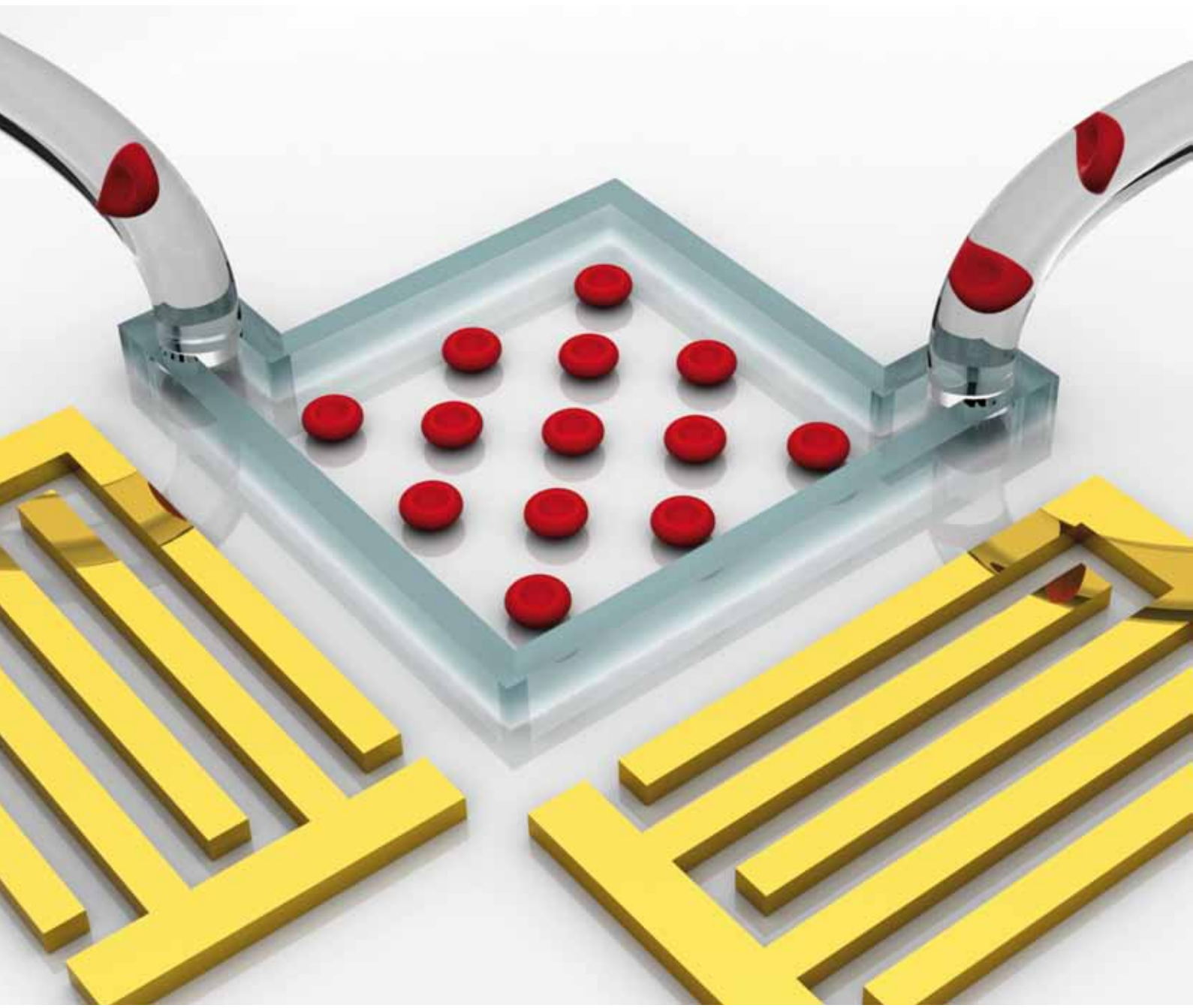

ISSN 1473-0197

RSC Publishing

Acoustic tweezers: patterning cells and microparticles using standing surface acoustic waves (SSAW)†

Jinjie Shi,[a] Daniel Ahmed,[a] Xiaole Mao,[ab] Sz-Chin Steven Lin,[a] Aitan Lawit[a] and Tony Jun Huang*[ab]

Received 29th May 2009, Accepted 22nd July 2009
First published as an Advance Article on the web 5th August 2009
DOI: 10.1039/b910595f

Here we present an active patterning technique named "acoustic tweezers" that utilizes standing surface acoustic wave (SSAW) to manipulate and pattern cells and microparticles. This technique is capable of patterning cells and microparticles regardless of shape, size, charge or polarity. Its power intensity, approximately 5×10^5 times lower than that of optical tweezers, compares favorably with those of other active patterning methods. Flow cytometry studies have revealed it to be non-invasive. The aforementioned advantages, along with this technique's simple design and ability to be miniaturized, render the "acoustic tweezers" technique a promising tool for various applications in biology, chemistry, engineering, and materials science.

Introduction

The ability to arrange cells and microparticles into desired patterns is critical for numerous biological studies and applications such as microarrays,[1,2] tissue engineering,[3,4] and regenerative medicine.[5,6] Researchers have developed a variety of patterning techniques such as microcontact printing,[7–9] optical tweezers,[10,11] optoelectronic tweezers,[12,13] magnetic tweezers,[14–16] electro-/dielectro-phoresis,[17–21] evanescent waves/plasmonics,[22,23] hydrodynamic flows,[24–32] and bulk acoustic wave-based acoustophoresis.[33–37]

The invention of optical tweezers[10,11] and developments in optofluidics[38–41] have spurned a new platform for manipulating and patterning micro/nanoscale objects with unprecedented precision. Chiou *et al.* demonstrated optoelectronic tweezers that featured not only the high precision of optical tweezers, but also achieved high throughput and low power consumption, with a power intensity approximately 1×10^5 times less than that of optical tweezers.[12] Most recently, Yang *et al.* demonstrated trapping and transporting dielectric nanoparticles as small as 75 nm using sub-wavelength slot waveguides.[42] Despite the impressive performance of such optics-based patterning and manipulating techniques, they require bulky, complicated optical setups, which are difficult to miniaturize. Techniques based on magnetic/electrical fields (such as magnetic tweezers, electrophoresis, and dielectrophoresis)[14–21] could serve as alternative solutions. These techniques are amenable to device miniaturization, but they have limited versatility. For example, magnetic tweezers require targets to be pre-labeled with magnetic materials. The recently developed bulk acoustic wave (BAW)-based acoustophoresis have shown promise in manipulating macro/micro particles regardless of their optical or electrical properties.[33–37] However, it is challenging to implement these BAW-based techniques with the existing fast-prototyping methods, such as soft lithography, that are widely used in microfluidics. Due to the limitations of the existing techniques, researchers are still searching for cell-patterning techniques that simultaneously meet specifications for miniaturization, versatility, throughput, speed, and power consumption.

A surface acoustic wave (SAW) is a sound wave that propagates along the surface of an elastic material.[43] When SAW propagates, most of its energy is confined within one to two wavelengths normal to the surface of the substrate.[43] This energy-confining characteristic makes SAW an energy-efficient tool for manipulating particles and biomaterials. Furthermore, SAW-based techniques are free of contamination, only introducing low-power mechanical vibrations to the suspension. Recently, researchers have demonstrated SAW-based mixing,[44] pumping,[45] concentration,[46] and particle focusing.[47] In this paper, we reveal an "acoustic tweezers" technique, in which microparticles and cells can be effectively patterned using standing surface acoustic waves (SSAW). This technique is versatile, non-invasive, and amenable to miniaturization, and its power consumption and speed compare favorably to those of existing active cell-patterning techniques.

Working mechanism

Fig. 1 illustrates the working principle of the "acoustic tweezers." The device consists of a polydimethylsiloxane (PDMS) microfluidic channel and a pair of interdigital transducers (IDTs) deposited on a piezoelectric substrate in a parallel (Fig. 1a) or orthogonal (Fig. 1b) arrangement. A solution of microparticles or cells is infused into the microchannel by a pressure-driven flow. Once the distribution of particles or cells stabilizes in the channel, a radio frequency (RF) signal is applied to both IDTs to generate two series of identical SAWs propagating either in the opposite (Fig. 1a) or orthogonal (Fig. 1b) direction. The interference of these two series of SAWs forms a SSAW, as well as

[a]*Department of Engineering Science and Mechanics, The Pennsylvania State University, University Park, PA, 16802, USA. E-mail: junhuang@psu.edu; Fax: +1 814-865-9974; Tel: +81 14-863-4209*
[b]*Department of Bioengineering, The Pennsylvania State University, University Park, Pennsylvania, 16802, USA*

† Electronic supplementary information (ESI) available: Including device fabrication, simulation of standing surface acoustic waves, flow cytometry measurements, qualitative force analysis and ID and 2D patterning of fluorescent microparticles. See DOI: 10.1039/b910595f

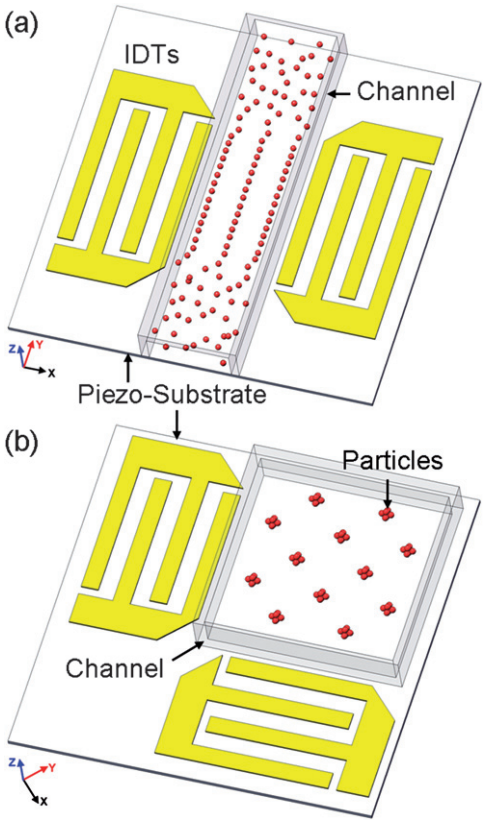

Fig. 1 Schematic of the SSAW-based patterning devices. (a) 1D patterning using two parallel IDTs. (b) 2D patterning using two orthogonal IDTs (the angle between the IDTs can be changed to achieve different patterns).

a periodic distribution of pressure nodes (with minimum pressure amplitude) and antinodes (with maximum pressure amplitude) on the substrate—the pressure distribution can be visualized from the simulated results (Fig. S2b and d, see detailed description in the ESI†).[48] When the SSAW encounters the liquid medium inside the channel, longitudinal-mode leakage waves are generated, causing pressure fluctuations in the medium.[44–47,49] These fluctuations lead to acoustic radiation forces that act on the suspended particles, moving them to the pressure nodes or antinodes in the SSAW field.[35,47,49] The primary acoustic force exerted on an object in a SSAW field can be expressed as[49]

$$F_r = -(\pi p_0^2 V_c \beta_w / 2\lambda) \cdot \phi(\beta,\rho) \cdot \sin(2kx) \quad (1)$$

$$\phi(\beta,\rho) = \frac{5\rho_c - 2\rho_w}{2\rho_c + \rho_w} - \frac{\beta_c}{\beta_w} \quad (2)$$

where p_0, λ, V_c are the acoustic pressure, wavelength, volume of the object, respectively; and ρ_c, ρ_w, β_c, β_w represent the density of the object, density of the medium, compressibility of the object, and compressibility of the medium, respectively. ϕ determines the balanced positions of the objects: if $\phi > 0$, the objects will aggregate at pressure nodes, and *vice versa*. In a one-dimensional (1D) SSAW field, the pressure nodes (or antinodes) are aligned in multiple lines, which are parallel to the wave fronts (Fig. S2b, ESI†), resulting in a 1D pattern of particles along these lines (Fig. 1a). In a two-dimensional (2D) SSAW field, instead of forming parallel lines, pressure nodes (or antinodes) form orthogonal 2D arrays (Fig. S2d, ESI†). Particles move towards nearby pressure nodes (or antinodes), forming 2D patterned aggregations (Fig. 1b).

Methods

Device fabrication and experimental procedure

There are three steps involved in the device fabrication (see Fig. S1 in the ESI†). Firstly, a thin layer of metal (Ti/Au, 50 Å/800 Å) was deposited on a photoresist-patterned lithium niobate substrate, followed by a lift-off process to form the IDTs. Secondly, polydimethylsiloxane (PDMS) microchannels were fabricated using standard soft lithography and mold-replica techniques. A pre-patterned silicon substrate was deep-etched to serve as the mold for PDMS channel fabrication. At last, the PDMS microchannel was aligned and bonded with the lithium niobate substrate, obtaining the desired device (see more details in the ESI†).

System setup

The SSAW-based patterning device was mounted on the stage of an inverted microscope (Nikon TE2000U), and solutions of fluorescent beads, bovine red blood cells (bRBC), and *E. coli* cells were injected into the device through a syringe pump (KDS210, Kd Scientific). An AC signal generated by an RF signal generator (Agilent E4422B) was split into two coherent signals, which were subsequently connected to the IDTs to generate SSAW. A CCD camera (CoolSNAP HQ2, Photometrics, Tucson, AZ) was connected to the microscope to capture the patterning processes. The power of the applied SAW was 200 mW (working area of 1 cm^2) in all of our experiments.

Sample preparation

Fluorescent (Dragon Green) polystyrene beads (11 760 000 beads mL^{-1}, ~1.9 μm in diameter, Bangs Laboratories), bRBCs (~6 μm in diameter, Innovative Research, Inc.), and *E. coli* cells (~800 nm in diameter, 1–3 μm in length) dyed with green fluorescence proteins (GFP) encoded plasmids were used in the patterning experiments. After the induced GFP expression, *E. coli* colonies were selected and re-suspended in PBS buffer to desired concentrations. Freshly-prepared *E. coli* cells, grown to mid-logarithmic phase in LB media, were divided into four parts: (a) pre-treated cells cultured for 12 h (Positive Control 1), (b) cells that flow through the microchannel without applying SSAW (Positive Control 2), (c) cells that experienced the SSAW patterning process in the microfluidic system (SSAW Sample), and (d) cells that were heated at 70 °C for 30 min (Negative Control). After the treatment, each group of cell culture was diluted in PBS buffer at a 1 : 100 ratio, and a 2 μL stock solution of $DiBAC_4(3)$ (Molecular probes, USA) was added to a 1 ml diluted cell suspension, resulting in a dye concentration of 5 μg mL^{-1}. The cells were then stained for 30 min before the flow cytometry measurement. The flow cytometry test was performed on a Beckman-Coulter XL-MCL flow cytometer using a blue-light (488 nm) excitation source. For each test, 2×10^4 cells were counted.

Results and discussion

Patterning of micro polystyrene beads

We first examined the "acoustic tweezers" technique in patterning fluorescent (Dragon Green) polystyrene beads of mean diameter 1.9 μm. Fig. 2 shows optical images of the 1D and 2D patterning devices. When the SSAW was applied, the beads aggregated at the pressure nodes, forming 1D and 2D patterns. The periods of the patterns were measured to be approximately 50 μm (1D pattern in Fig. 2c) and 140 μm (2D pattern in Fig. 2d). The experimentally measured data matched well with the simulated results (Fig. S2 b and d, ESI†), which predicted that the period of the 1D pattern would be half of the SAW working wavelength (50 μm) and that the period of the 2D pattern would be $\sqrt{2}/2$ times the SAW working wavelength (141 μm). The size of the bead aggregations at the pressure nodes (Fig. 2c and 2d) can be tuned by altering the applied power. Higher power leads to larger acoustic radiation forces, resulting in close-packed bead aggregations.

Patterning of cells

We further proved that the "acoustic tweezers" technique can readily be used to pattern different types of cells—bRBC in Fig. 3a and *E. coli* cells in Fig. 3b. These results verify the versatility of our technique as the two groups of cells differ significantly in both shape (spherical bRBC *vs.* rod-shaped *E. coli*) and size (~6 μm *vs.* ~1 μm). Furthermore, the patterning performance is independent of the particles' electrical/magnetic/optical properties. One concern about this technique is that the mechanical forces generated by the acoustic waves may potentially damage cells during the patterning process. For example, BAW has been widely used in ultrasonic imaging, cell sonoporation, and ultrasound-enhanced drug delivery.[50–52] In comparison to these BAW-based techniques, which operate at larger power intensities (2000–6000 W m^{-2}) for tens of minutes or even hours without significantly reducing cell viability, our "acoustic tweezers" technique used nominal power intensity and took only seconds to drive cells to pressure nodes. Damages caused by acoustic forces during this period should be trivial. Once the cells

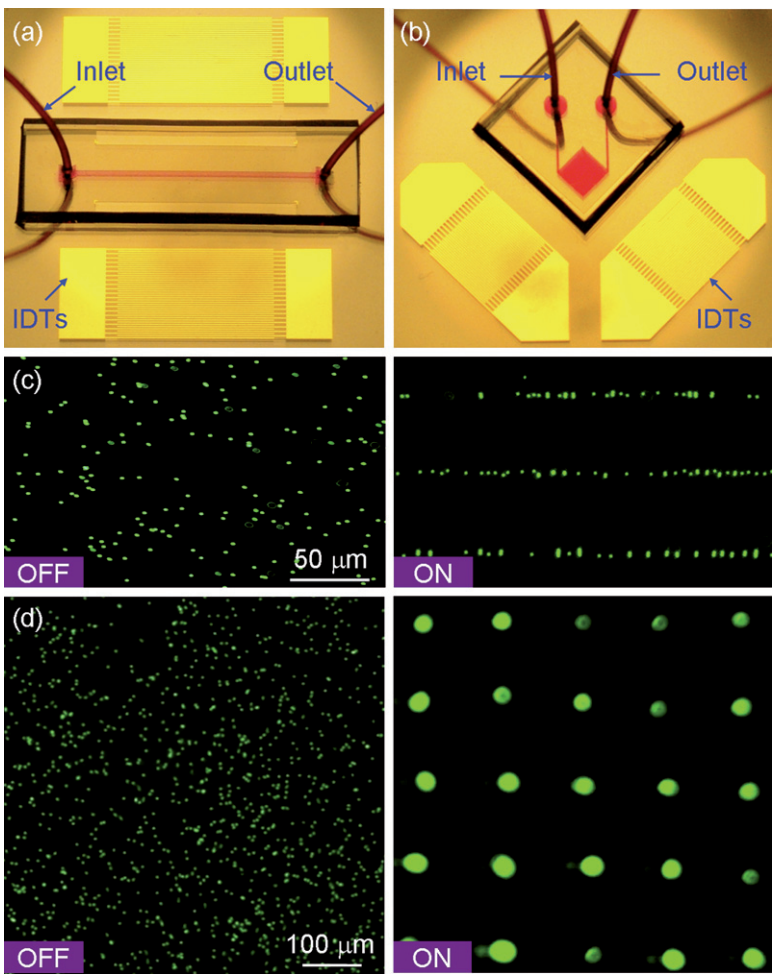

Fig. 2 Patterning of fluorescent polystyrene microbeads. Optical images of the "acoustic tweezers" devices used in (a) 1D and (b) 2D patterning experiments, respectively. (c) Distribution of the microbeads before and after the 1D patterning process. The microchannel (width = 150 μm and depth = 80 μm) covered three lines of pressure nodes of the generated SSAW. The wavelength of SAW was 100 μm (see Supplementary Video 1, ESI†). (d), Distribution of the microbeads before and after the 2D patterning process. The SAW wavelength was 200 μm.

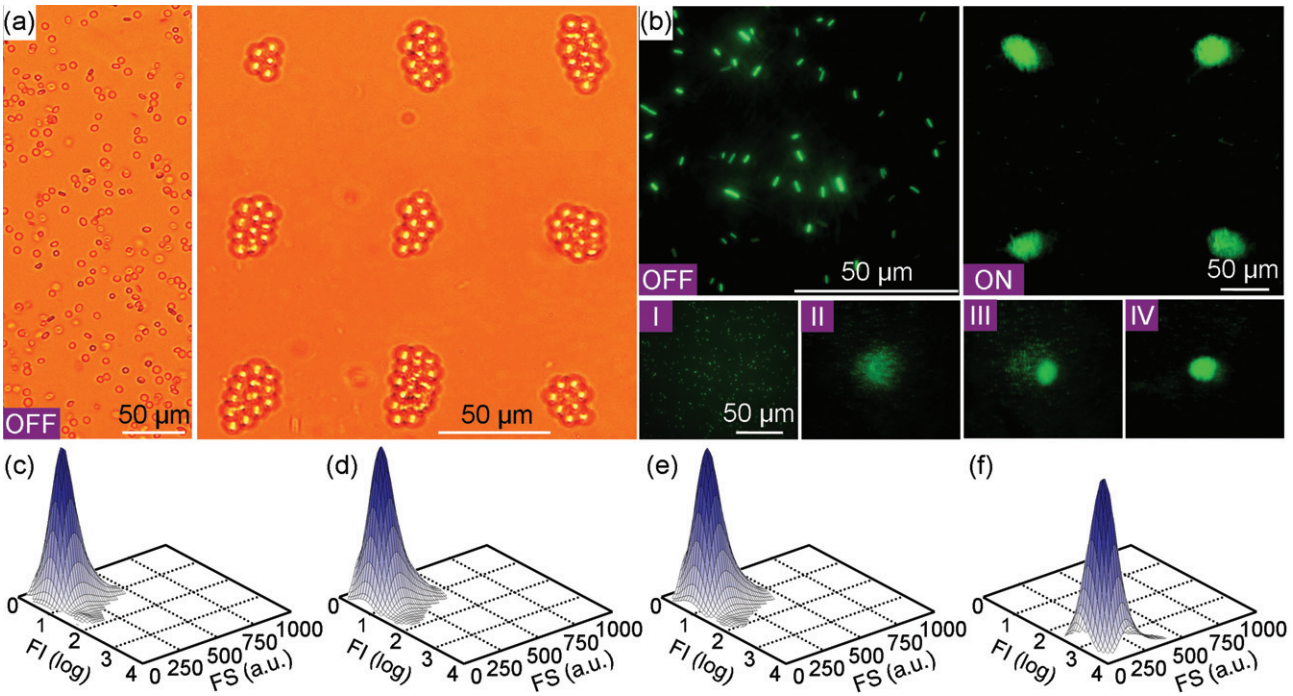

Fig. 3 SSAW-based cell patterning. (a) Patterning of bRBC. The wavelength of the applied SAW was 100 μm. (b) Patterning of *E. coli* cells pretreated with Dragon Green fluorescent dyes. The wavelength of the applied SAW was 300 μm (see Supplementary Video 2, ESI†). I ~ IV shows the dynamic process of *E. coli* cells aggregate at a pressure node. (c–f), Flow cytometric histograms (DiBAC4(3) fluorescent light intensity (FI) *vs.* forward scattering (FS)) for different cell types. (c) *E. coli* cells cultured for 12 h (Positive Control 1); (d) *E. coli* cells that passed through a microchannel without applying SSAW (Positive Control 2); (e) *E. coli* cells that experienced the SSAW-based patterning process in a microchannel (SSAW Sample); and (f) *E. coli* cells heated at 70 °C for 30 min (Negative Control).

reached the pressure nodes, the acoustic pressures, and thus acoustic forces applied to the cells, were nearly zero; cells were steadily patterned in the "wells" defined by the pressure gradients around the pressure nodes. At the same time, the pressure oscillations inside the patterned cells (at pressure nodes) are also nearly zero, minimizing the heat generation. These characteristics suggest that the "acoustic tweezers" technique would be non-invasive to cells.

In order to confirm the non-invasive nature of our technique, we studied the integrity of the cell membranes before and after the patterning process. We used a membrane-potential-sensitive dye, $DiBAC_4(3)$ (bis-(1,3-dibarbituric acid)-trimethine oxanol), as an indicator for cell viability. $DiBAC_4(3)$ is an anionic lipophilic fluorescent dye which is found mainly in the outer cytoplasmic membranes of intact cells.[47] It enters the cell body and accumulates in the cytoplasm when the cell membrane is damaged. Thus, the amount of dye accumulation, which is indicated by the average fluorescent intensity (FI), can be used to quantify the degree of membrane disruption caused by our technique. We performed flow cytometry experiments to quantitatively analyze the viability of cells, in which FI and the forward scattering (FS) signals represented the cell viability and size distribution, respectively.[53] As shown in Fig. 3c–e, the *E. coli* cells after the SSAW patterning process (average FI = 0.536; Fig. 3e) exhibited distribution peaks almost identical to those of the cells prior to the pattering process (positive controls of average FI = 0.530–0.536; Fig. 3c and 3d). On the other hand, the cells incubated at 70 °C for 30 min (negative control; Fig. 3f) exhibited a much higher FI (2.2), implying that the cell membranes were severely damaged. These results (as detailed in Supplementary Table 1, ESI†) confirm that our SSAW-based "acoustic tweezers" technique is non-invasive.

Quantitative force analysis

The behavior of cells or other objects in a SSAW field can be predicted *via* theoretical force analyses. The primary forces involved in the SSAW patterning process are as follows: (1) acoustic radiation forces;[35,44–47,49] (2) viscous forces; (3) buoyant forces; and (4) gravity. Among these forces, buoyant forces are typically balanced by gravitational forces as they are of similar magnitudes and in opposite directions. Fig. 4a shows the dependence of these forces on particle size. It reveals that when the diameters of the particles are >1 μm, acoustic forces dominate under the applied power intensity. Fig. 4b shows that when the SAW wavelength is smaller than 100 μm, the acoustic forces acting upon the targets (polystyrene beads with diameter of 1.9 μm, bRBC, and *E. coli* cells) are significantly stronger than the viscous forces. In this study, all the particles were trapped at the pressure node, where the acoustic force was minimal and particles were immobilized due to the force gradient around the pressure node. Fig. 4c shows the acoustic force distribution within a half wavelength region centered at a pressure node. The results show that the acoustic forces change sinusoidally and point to the pressure node, forming a trapping well (inset of Fig. 4c). To release a particle from the trapping well, one must

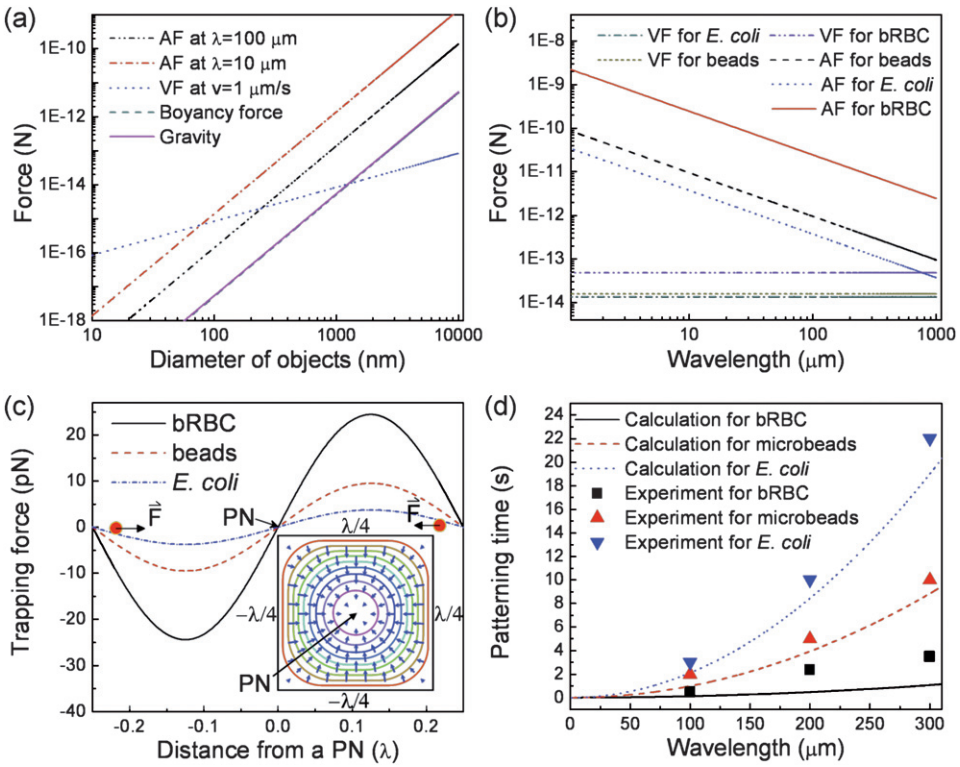

Fig. 4 Theoretical analyses. (a) Size dependence of acoustic force (AF), viscous force (VF), buoyant force, and gravitational force. (b), Dependence of AF and VF on the working wavelength for different objects. (c) The distribution of trapping force around a pressure node (PN). The forces on beads and E. coli are magnified 10 times for clear visualization. The inset indicates the force vectors and equal force contours around the PN. The SAW wavelength was 100 μm. (d) Calculated and experimental patterning time. The SAW intensity was 2000 W m^{-2}, and the particles speed was 1 μm s^{-1} in VF calculation.

overcome the maximum acoustic force in the field (25 pN for bRBC). By increasing the operation power or reducing the SAW working wavelength, one can further increase the stiffness of the trapping well built by the acoustic forces gradient around the pressure nodes or antinodes, making it possible to manipulate and pattern nanoscale particles.[35,42,44–47,49] In addition, our experimental and calculated results (Fig. 4d) show that the process for patterning polystyrene beads and bRBC takes less than 3 s, a speed faster than those of the previously reported studies.[12,17,18,25] Detailed description of the theoretical model used in Fig. 4 can be found in the ESI.†

In conclusion, we have demonstrated a SSAW-based "acoustic tweezers" technique that enables one to actively pattern cells and microparticles. This technique does not require pre-treatments on the substrates or cells/microparticles. It is applicable to virtually any type of cell/microparticle regardless of size, shape, or electrical/magnetic/optical properties. We verified this versatility by patterning polystyrene beads, bRBC, and *E. coli* cells. The required power intensity of acoustic tweezers (2000 W m^{-2}) is $\sim 5 \times 10^5$ times lower than that of optical tweezers (10^9 W m^{-2}) and compares favorably to those of other patterning methods.[12,23] Such a low power intensity also contributes to the technique's non-invasive nature, as confirmed by our cell viability studies. With its advantages in versatility, miniaturization, power consumption, speed, and technical simplicity, our "acoustic tweezers" technique is a powerful tool for applications such as tissue engineering, microarray, cell studies, and drug screening and discovery.

Acknowledgements

We thank Dr Bernhard R. Tittmann, Dr Kenji Uchino, Subash Jayaraman and Seyit Ural for help with equipments, and Yanjun Liu and Thomas R. Walker for helpful discussion. This research was supported by National Science Foundation (ECCS-0824183, ECCS-0801922, and ECCS-0609128) and the Penn State Center for Nanoscale Science (MRSEC). Components of this work were conducted at the Penn State node of the NSF-funded National Nanotechnology Infrastructure Network.

References

1 C. J. Flaim, S. Chien and S. N. Bhatia, *Nat. Methods*, 2005, **2**, 119–125.
2 D. B. Wheeler, A. E. Carpenter and D. M. Sabatini, *Nat. Genet.*, 2005, **37**, S25–S30.
3 M. M. Stevens, M. Mayer, D. G. Anderson, D. B. Weibel, G. M. Whitesides and R. Langer, *Biomaterials*, 2005, **26**, 7636–7641.
4 A. Tourovskaia, X. Figueroa-Masot and A. Folch, *Lab Chip*, 2005, **5**, 14–19.
5 C. Smith, *Nature*, 2007, **446**, 219–222.
6 S. R. Khetani and S. N. Bhatia, *Nat. Biotechnol.*, 2007, **26**, 120–126.
7 A. Hernard and et al, *Langmuir*, 1998, **14**, 2225–2229.
8 E. S. Douglas, R. A. Chandra, C. R. Bertozzi, R. A. Mathies and M. B. Francis, *Lab Chip*, 2007, **7**, 1442–1448.

9 S. Pernagallo, J. J. Diaz-Mochon and M. Bradley, *Lab Chip*, 2009, **9**, 397–403.
10 A. Ashkin, J. M. Dziedzic and T. Yamane, *Nature*, 1987, **330**, 769–771.
11 D. G. Grier, *Nature*, 2003, **424**, 810–816.
12 P. Y. Chiou, A. T. Ohta and M. C. Wu, *Nature*, 2005, **436**, 370–372.
13 H. Hwang and J.-K. Park, *Lab Chip*, 2009, **9**, 199–206.
14 H. Lee, A. M. Purdon and R. M. Westervelt, *Appl. Phys. Lett.*, 2004, **85**, 1063–1065.
15 K. Ino, M. Okochi, N. Konishi, M. Nakatochi, R. Imai, M. Shikida, A. Ito and H. Honda, *Lab Chip*, 2008, **8**, 134–142.
16 H. Lee, Y. Liu, D. Ham and R. M. Westervelt, *Lab Chip*, 2007, **7**, 331–337.
17 N. Mittal, A. Rosenthal and J. Voldman, *Lab Chip*, 2007, **7**, 1146–1153.
18 C.-T. Ho, R.-Z. Lin, W.-Y. Chang, H.-Y. Chang and C.-H. Liu, *Lab Chip*, 2006, **6**, 724–734.
19 R. S. Thomas, H. Morgan and N. G. Green, *Lab Chip*, 2009, **9**, 1534–1540.
20 T.-H. Wang, Y. Peng, C. Zhang, P. K. Wong and C.-M. Ho, *J. Am. Chem. Soc.*, 2005, **127**, 5354–5359.
21 M. Abdelgawad, M. W. L. Watson and A. R. Wheeler, *Lab Chip*, 2009, **9**, 1046–1051.
22 S. Kawata and T. Sugiura, *Opt. Lett.*, 1992, **17**, 772–774.
23 M. Righini, A. S. Zelenina, C. Girard and R. Quidant, *Nat. Phys.*, 2007, **3**, 477–480.
24 C.-H. Hsu, D. Di Carlo, C. Chen, D. Irimia and M. Toner, *Lab Chip*, 2008, **8**, 2128–2134.
25 D. Di Carlo, L. Y. Wu and L. P. Lee, *Lab Chip*, 2006, **6**, 1445–1449.
26 M. Deutsch, A. Deutsch, O. Shirihai, I. Hurevich, E. Afrimzon, Y. Shafran and N. Zurgil, *Lab Chip*, 2006, **6**, 995–1000.
27 A. Manbachi, S. Shrivastava, M. Cioffi, B. G. Chung, M. Moretti, U. Demirci, M. Yliperttula and A. Khademhosseini, *Lab Chip*, 2008, **8**, 747–754.
28 M. C. Park, J. Y. Hur, K. W. Kwon, S.-H. Park and K. Y. Suh, *Lab Chip*, 2006, **6**, 988–994.
29 A. Azioune, M. Storch, M. Bornens, M. Théry and M. Piel, *Lab Chip*, 2009, **9**, 1640–1642.
30 K. Yoshimoto, M. Ichino and Y. Nagasaki, *Lab Chip*, 2009, **9**, 1286–1289.
31 X. Mao, J. R. Waldeisen, B. K. Juluri and T. J. Huang, *Lab Chip*, 2007, **7**, 1303–1308.
32 X. Mao, S. S. Lin, M. I. Lapsley, J. Shi, B. K. Juluri and T. J. Huang, *Lab Chip*, 2009, **9**, 2050–2058.
33 O. Manneberg, B. Vanherberghen, B. Önfelt and M. Wiklund, *Lab Chip*, 2009, **9**, 833–837.
34 A. Nilsson, F. Petersson, H. Jönsson and T. Laurell, *Lab Chip*, 2004, **4**, 131–135.
35 T. Laurell, F. Petersson and A. Nilsson, *Chem. Soc. Rev.*, 2007, **36**, 492–506.
36 F. Petersson, L. Aberg, A. M. Sward-Nilsson and T. Laurell, *Anal. Chem.*, 2007, **79**, 5117–5123.
37 M. Wiklund, C. Günther, R. Lemor, M. Jäger, G. Fuhr and H. M. Hertz, *Lab Chip*, 2006, **6**, 1537–1544.
38 D. Psaltis, S. R. Quake and C. H. Yang, *Nature*, 2006, **442**, 381–386.
39 L. Dong, A. K. Agarwal, D. J. Beebe and H. Jiang, *Nature*, 2006, **442**, 551–554.
40 X. Mao, S. S. Lin, C. Dong and T. J. Huang, *Lab Chip*, 2009, **9**, 1583–1589.
41 X. Mao, J. R. Waldeisen and T. J. Huang, *Lab Chip*, 2007, **7**, 1260–1262.
42 A. H. J. Yang, S. D. Moore, B. S. Schmidt, M. Klug, M. Lipson and D. Erickson, *Nature*, 2009, **457**, 71–75.
43 C. Campbell and J. C. Burgess, *J. Acoust. Soc. Am.*, 1991, **89**, 1479–1480.
44 T. Frommelt, M. Kostur, M. Wenzel- Schäfer, P. Talkner, P. Hänggi and A. Wixforth, *Phys. Rev. Lett.*, 2008, **100**, 034502.
45 Z. Guttenberg, H. Müller, H. Habermüller, A. Geisbauer, J. Pipper, J. Felbel, M. Kielpinski, J. Scriba and A. Wixforth, *Lab Chip*, 2005, **5**, 308–317.
46 M. K. Tan, J. R. Friend and L. Y. Yeo, *Lab Chip*, 2007, **7**, 618–625.
47 J. Shi, X. Mao, D. Ahmed, A. Colletti and T. J. Huang, *Lab Chip*, 2008, **8**, 221–223.
48 S. Oberti, A. Neild and J. Dual, *J. Acoust. Soc. Am.*, 2007, **121**, 778–785.
49 K. Yosioka and Y. Kawasima, *Acustica*, 1955, **5**, 167–173.
50 M. D. Sherar, M. B. Noss and F. S. Foster, *Nature*, 1987, **330**, 493–495.
51 S. Mitragotri, D. Blankschtein and R. Langer, *Science*, 1995, **269**, 850–853.
52 V. Zderic, J. I. Clark and S. Vaezy, *J. Ultrasound Med.*, 2004, **23**, 1349–1359.
53 R. I. Jepras, J. Carter, S. C. Pearson, F. E. Paul and M. J. Wilkinson, *Appl. Environ. Microbiol.*, 1995, **61**, 2696–2701.